Residual thermal desorption study of the room-temperature-formed Sb/Si(111) interface

Vinod Kumar Paliwal,[1,2] A. G. Vedeshwar,[2] and S. M. Shivaprasad[1,*]
[1]*Surface Physics Group, National Physical Laboratory, New Delhi-110 012, India*
[2]*Department Of Physics & Astrophysics, University of Delhi, Delhi-110007, India*
(Received 23 May 2002; revised manuscript received 11 September 2002; published 5 December 2002)

This paper addresses issues of the subtle kinetic changes on the superstructural phase formation in the technologically important Sb/Si system. The thermal stability of the room-temperature (RT) deposited Sb on a (7×7) reconstructed Si(111) surface by Auger electron spectroscopy (AES), low-energy electron diffraction (LEED), and electron energy-loss spectroscopy (EELS) is reported. At a very low Sb flux rate of 0.03 ML/min Sb uptake shows that it grows in the Frank–van der Merwe mode yielding a (1×1) LEED pattern for coverages of 1.0 ML and above. On annealing, AES shows that initially Sb adatoms agglomerate into large islands on top of a stable monolayer, before the Sb islands desorb in the temperature range of 350° C–480° C , to leave a sharp (1×1) stable Sb monolayer. Monolayer desorption from about 650° C results in several surface phases such as $d(2\times1)$, (5×5), $(\sqrt{3}\times\sqrt{3}$-$R30°)$ and $(5\sqrt{3}\times5\sqrt{3}$-$R30°)$. The (5×5) at 0.4 ML and the $(5\sqrt{3}\times5\sqrt{3}$-$R30°)$ at 0.2 ML are novel phases observed only during this desorption route. However, the 0.5–0.7-ML $(5\sqrt{3}\times5\sqrt{3}$-$R30°)$ phase, observed while desorbing from a 1.0-ML $(\sqrt{3}\times\sqrt{3}$-$R30°)$ initial phase, is not observed here. The EELS studies show the differences in the surface-related electronic features of the various superstructural phases. The results demonstrate the differences in the superstructural phase formation due to differences in the formation pathways adopted.

DOI: 10.1103/PhysRevB.66.245404 PACS number(s): 68.35.−p, 61.14.Hg, 79.20.Uv

I. INTRODUCTION

Studies of the kinetic control of submonolayer metal adsorption on Si(111) and (100) surfaces have resulted in interesting results regarding growth modes, superstructural phase formation, and interfacial interactions.[1–5] Though the conditions of growth cause formidable issues of repeatability, they also provide a potential to form several stable interfacial phases with novel electronic properties. Motivated by the need to form sharp dopant profiles,[6] studies of the adsorption of group-III and -V metals on single-crystal silicon surfaces have been intensely pursued.[1] In this paper we report the results of the study of the thermal stability of a room-temperature (RT) -formed Sb/Si(111) system. The Sb/Si interface is one of the most intensely probed systems, due to the technological importance both in the formation of δ-doped systems[7,8] and in surfactant (Sb)-mediated Ge/Si heteroepitaxy.[9,10] Our recent study,[11] and those of others,[12–14] has shown that the adsorption of Sb at various substrate temperatures of the (7×7) reconstructed Si(111) surface results in several surface phases such as $(\sqrt{3}\times\sqrt{3}$-$R30°)$ at 1.0 ML [written as $(\sqrt{3}\times\sqrt{3})$ below], three-domain $d(2\times1)$ at 0.85 ML [$d(2\times1)$ below], $(5\sqrt{3}\times5\sqrt{3}$-$R30°)$ at 0.5–0.7-ML [$(5\sqrt{3}\times5\sqrt{3})$ below], $(\sqrt{3}\times\sqrt{3}$-$R30°)$ at 0.33-ML, and (7×7) at 0.1-ML Sb coverages. Among these, the atomic structures of the 1.0-ML $(\sqrt{3}\times\sqrt{3})$ (as Sb trimers) and (2×1) (Sb zigzag chains) have been established conclusively.[13,15] The structure of 0.6-ML $(5\sqrt{3}\times5\sqrt{3})$ is understood as a (5×5) dimer-adatom-stacking fault (DAS) structure with different compositions of the adatom and rest-atom layers within the different unit-cell halves.[15–17] Recent studies of Saranin *et al.*[18] have shown that the $(5\sqrt{3}\times5\sqrt{3})$ does not have a definite composition since the Sb atoms partially substitute for the boundary dimers in the basic (5×5) structure, and thus can exist in the Sb coverage range of 0.41–0.77 ML. The $(\sqrt{3}\times\sqrt{3})$ at 0.33 ML has been observed by Elswijk *et al.*,[13] in small domains coexisting with (7×7) and disordered (7×7) phases. In our previous paper,[11] we not only confirmed the above superstructures but also revised the prevailing phase diagram. During the studies we realized the need for a systematic and careful study to highlight the effects of subtle changes in the kinetics on the superstructure formation of this technologically important system.

Earlier Sb adsorption-desorption studies[19] have shown that the first-monolayer Sb adsorbs as Sb_4 and dissociates quickly on Si surfaces. Sb_4 desorption comes from the multilayers, while the Sb monolayer chemisorbed on the Si(111) surface desorbs as Sb. In this report we adsorb Sb of several coverages at RT at very low flux rates and anneal the system to different temperatures and observe the residual system. By *in situ* Auger electron spectroscopy (AES), low energy electron diffraction (LEED), and electron energy-loss spectroscopy (EELS), we observe that epitaxial Sb layers, upon annealing, agglomerate into large islands on top of a stable (1×1) monolayer. At higher temperatures the islands desorb, leaving a stable monolayer. Further annealing causes the monolayer desorption, during which we observe a variety of stable superstructures of submonolayer coverages.

II. EXPERIMENT

The experiments are performed *in situ* in an ultra high vacuum (UHV) system (Varian VT-112) with a base pressure of 3×10^{-11} torr with four-grid LEED optics for probing the structures and a cylindrical mirror analyzer for AES and EELS measurements. The Si surface is chemically cleaned by a modified Shiraki process[20] before inserting it into UHV. In vacuum, the sample is flashed at 1200° C for several sec-

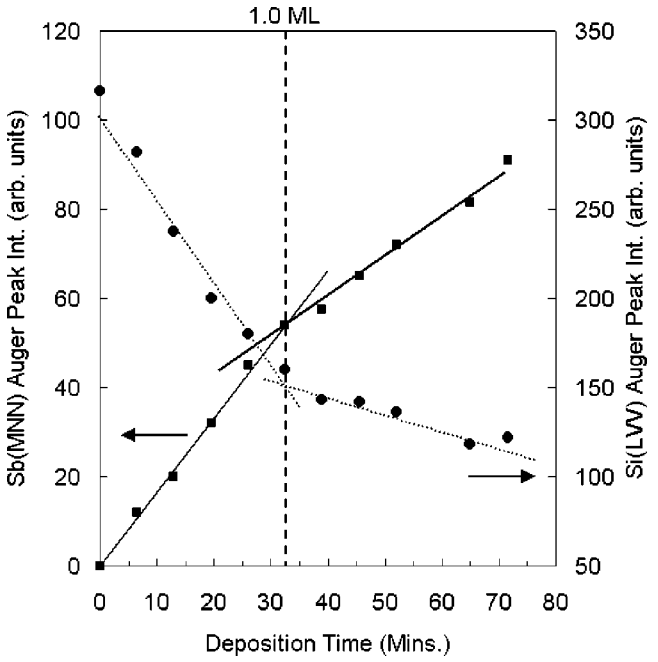

FIG. 1. Auger uptake curve showing Frank–van der Merwe growth mode, with breaks in slope for Sb(MNN) and Si(LVV) peak intensities at a deposition time of about 33 min corresponding to 1.0-ML Sb coverage.

onds and cooled gradually to RT to obtain a very clean (7×7) surface, as ascertained by AES and LEED. Sb is evaporated from a homemade Ta Knudsen cell at desired flux rates. The substrate, held by Ta clamps, is resistively heated and the temperature is measured with an error of $\pm 20°$ C by a calibrated W-Re thermocouple and an optical pyrometer. We report here studies of the growth of submonolayer coverages of Sb. One monolayer is defined as the density of a bulk truncated Si(111) surface which is 7.85×10^{14} atoms/cm^2. Thorough degassing ensures that the base pressure rises to a maximum of 8×10^{-10} torr even during extended Sb adsorption. Annealing was done either by radiative heating by a proximal Ta filament, or by resistively heating the sample to the desired temperature, holding it there for 2 min, and cooling it to RT before making EELS, AES, and LEED measurements.

III. RESULTS AND DISCUSSION

On the clean (7×7) reconstructed Si(111) surface held at RT, Sb is adsorbed at a rate of 0.03 ML/min. The Sb uptake is shown in Fig. 1, where the Sb(MNN) and Si(LVV) Auger signals are plotted as a function of deposition time. Since the Sb(MNN) Auger electrons originating from the first monolayer are attenuated due to the presence of the second-layer adatoms[21] and those of Si(LVV) due to the Sb overlayer, the curve in Sb(MNN) and Si(LVV) show a break in slope at about 33 min of deposition time thus giving us a calibration for our Sb flux rate as 0.03 ML/min. We identify the break in this uptake curve by a method suggested by Stampanoni *et al.*[22] We have confirmed that the break point corresponds to 1.0 ML by comparing the Auger ratio of this and by attaining the $(\sqrt{3}\times\sqrt{3})$ symmetry at 1.0 ML obtained by adsorbing Sb onto a Si substrate held at around 650° C. This result indicates that for RT adsorption at very low flux rates, the overlayer evolves in the Frank–van der Merwe (FM) growth mode for several layers (we have shown only the first two layers in Fig. 1). The (7×7) LEED of clean Si(111) changes to (1×1) for coverages of 1.0 ML and above [see Fig. 3(a) below]. Similar layer-by-layer (FM) growth has been reported by Metzger and Allen[23] for the Sb/Si(111) system. However, Cuberes *et al.*[24] observe an island type of growth, even for coverages as low as 0.25 ML. This discrepancy could be due to differences in the Sb flux rates (0.5 ML/min used by Cuberes *et al.*) and other experimental conditions.

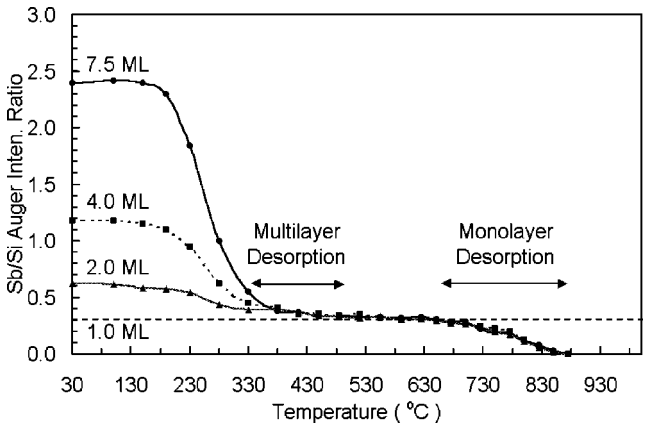

FIG. 2. Sb/Si Auger ratio as a function of temperature for three coverages, viz., 2.0, 4.0, and 7.5 ML. The dashed straight line at the 0.32 ratio corresponds to 1.0-ML Sb coverage. The temperature ranges, shown by double-sided arrows, mentioned as multilayer desorption, and monolayer desorption are taken from Metzger and Allen (Ref. 23).

The thermal stability of this layer-by-layer grown system is seen in Fig. 2 which plots the Auger ratio of Sb(MNN) at 454 eV and Si(LVV) at 92 eV, as the RT adsorbed system is annealed to increasing temperatures. It is evident from the figure that the Auger ratio hardly changes up to a temperature of 180° C. At around 350° C, it sharply falls to a value corresponding to a coverage of about 1.0 ML in all the three coverage cases studied, viz., 2.0, 4.0, and 7.5 ML. The initial (1×1) LEED pattern [Fig. 3(a)] which had a strong background assumes a sharp (1×1) pattern at the stable monolayer [Fig. 3(b)], after the multilayer desorption. To understand this behavior we refer to the pioneering work of Metzger and Allen,[23] where mass spectrometric thermal-desorption studies were performed. From this and other[19] studies, it is clear that the multilayer Sb, corresponding to only Sb-Sb bonds, desorbs as Sb_4 in the temperature range of 350° C–480° C, with a desorption energy of 1.49 eV. Thus, the fall in the Auger ratio in the temperature range of 180° C–350° C (before the multilayer desorption takes place) can be predominantly attributed to the agglomeration of Sb adatoms into large islands on top of a stable Sb monolayer. From the previous conventional thermal-desorption spectroscopy (TDS) study of Metzger and Allen[23] and those of Andrieu and Arnaud d'Avitaya,[19] it can be safely inferred

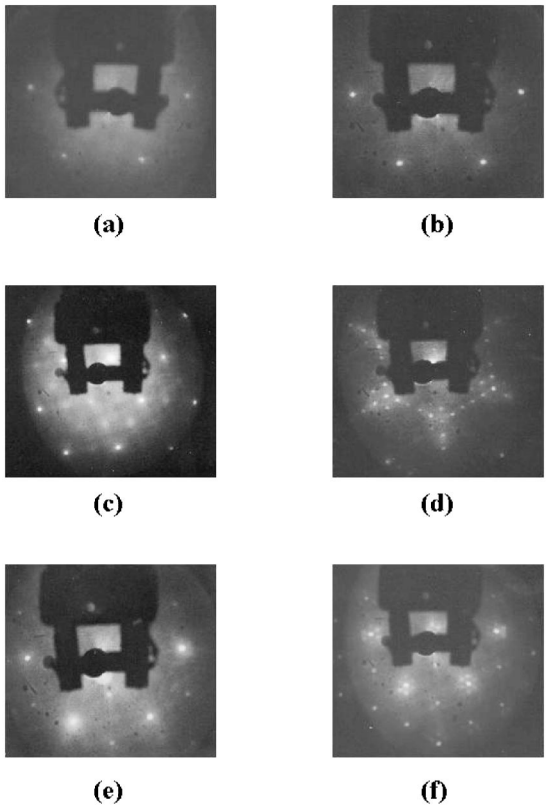

FIG. 3. LEED pattern for several surface phases observed during the thermal stability study. LEED pattern obtained for several Sb/Si(111) interfacial phases: During Sb adsorption (a) (1×1) for 2.1 ML (at 53 eV), and during residual thermal desorption (b) (1×1) for 1.1 ML (at 53 eV), (c) $d(2\times1)$ for 0.85 ML (at 83 eV), (d) (5×5) for 0.4 ML (at 53 eV), (e) $(\sqrt{3}\times\sqrt{3}$-$R30°)$ for 0.33 ML (at 53 eV), and (f) $(5\sqrt{3}\times5\sqrt{3}$-$R30°)$ for 0.2 ML (at 63 eV).

that there is hardly any appreciable desorption or bulk diffusion of Sb at temperatures below 350° C. To get only a qualitative picture, assuming that this thermally activated agglomeration into large islands follows an Arrhenius type of behavior, we calculate the Sb diffusion energy for agglomeration to be less than 0.2 eV for all three coverages studied. The smallness of the energies involved suggests that the growth parameters can strongly influence the growth modes in this system.

In the temperature range 480° C–650° C, the (1×1) LEED at 1.0 ML [shown in Fig. 3(b)] changes to a $d(2\times2)$ plus (1×1) pattern identified earlier as three-domain $d(2\times1)$,[13] as the coverage reduces to about 0.9 ML. At temperatures greater than 650° C, the Auger ratio further reduces, finally resulting in only a substrate signal and a (7×7) LEED at 880° C. In this 650° C–880° C temperature range, the Sb monolayer that was strongly bound to the substrate desorbs with a desorption energy of 2.46 eV.[23] As the monolayer Sb adatoms desorb from preferential sites, long-range order persists and several LEED patterns are seen, as shown in Fig. 3. The $d(2\times1)$ pattern [Fig. 3(c)] results in a (5×5) LEED [Fig. 3(d)] when the Auger ratio corresponds to a coverage of 0.4 ML. This LEED pattern changes to a $(\sqrt{3}\times\sqrt{3})$ phase [Fig. 3(e)] at 0.33-ML Sb coverage, while it

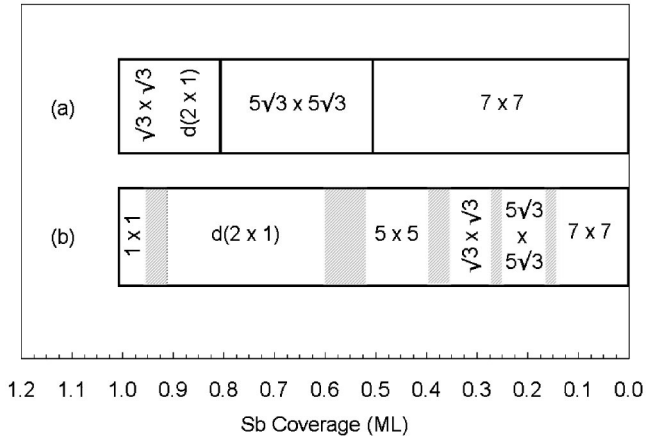

FIG. 4. Phase diagram of the desorption route: (a) Starting from the $(\sqrt{3}\times\sqrt{3}$-$R30°)$ phase at 1.0 ML and (b) starting from a (1×1) phase at 1.0 ML for Sb/Si(111) system. The hashed portions in (b) show regions of crossover.

forms $(5\sqrt{3}\times5\sqrt{3})$ at a coverage of 0.2 ML [Fig. 3(f)]. As the Auger ratio corresponds to 0.1 ML, a (7×7) Sb/Si phase is seen, to ultimately result in a sharp (7×7) clean Si(111) surface. It is interesting to note that the $(\sqrt{3}\times\sqrt{3})$ phase at 1.0 ML and the $(5\sqrt{3}\times5\sqrt{3})$ at around 0.6 ML reported by us[11] and others[12–14] are not seen in these thermal stability studies, which we attribute to the differences in the adopted pathways. On the other hand, the novel (5×5) at 0.4-ML and the $(5\sqrt{3}\times5\sqrt{3})$ at 0.2-ML phases are seen only in these desorption studies, while they were not evident in adsorption studies done while the substrate was held at corresponding temperatures.

Figure 4 shows the various phases observed by Park *et al.*[12] and Andrieu,[14] obtained from desorption starting from an initial $(\sqrt{3}\times\sqrt{3})$ 1.0-ML phase [Fig. 4(a)], and the present results of the phases starting from a RT formed (1×1) phase [Fig. 4(b)]. These previous studies starting from a $(\sqrt{3}\times\sqrt{3})$ 1.0-ML phase in the course of desorption have observed three-domain $d(2\times1)$ followed by $(5\sqrt{3}\times5\sqrt{3})$ at 0.5-0.7 ML and the gradual restoration of (7×7). We have also performed desorption studies starting from the $(\sqrt{3}\times\sqrt{3})$ 1.0-ML phase, and have essentially reproduced the same results shown in Fig. 4(a). It is clear from this figure that since in the present case we have started our desorption studies [Fig. 4(b)] from a RT adsorbed (1×1) phase (at 1.0 ML and higher coverages), we observe different superstructural phases, clearly demonstrating the differences due to the pathways adopted. It may be recalled here that, we have reported[2] differences in the atomic arrangements of Ag, at the same substrate temperatures, due to different formation pathways adopted.

The several surface phases evolved during the thermal treatment are quite stable at the respective temperatures. The electronic properties of these phases are studied by monitoring the electron energy losses to single and collective electron excitations. The EELS spectra shown in Fig. 5, which is the first such study on the Sb/Si system to the best of our knowledge, are taken in the second derivative mode at 250-eV primary beam energy, of each of the phases ob-

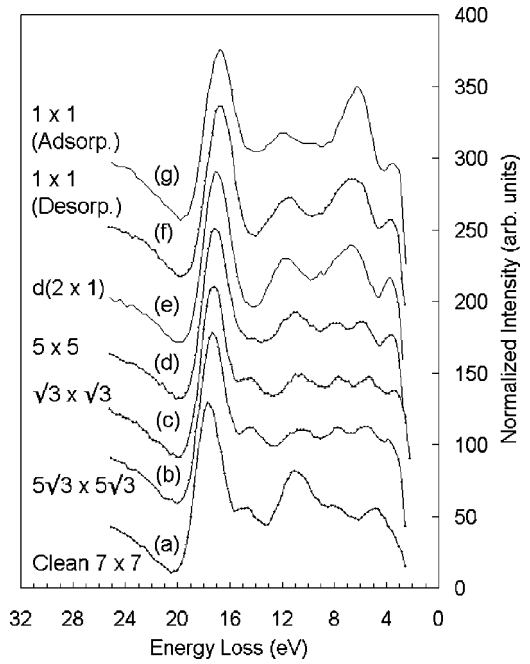

FIG. 5. EELS spectra of different surface phases, observed during desorption, in the d^2N/dE^2 mode is shown for primary beam energy of 250 eV.

served. The clean Si(111)-(7×7) EELS in Fig. 5(a) shows sharp peaks at 17.5, 14.5, 11.0, 8.0, and 4.7 eV in concurrence with earlier studies.[25] The 17.5-eV peak is attributed to the electron energy losses to the bulk plasmon while the 11.0-eV peak corresponds to the loss to surface plasmons. The peaks at 14.5 eV and 8.0 eV are related to the surface states that manifest the (7×7) reconstruction, while the 4.7-eV peak is associated with interband transitions at 3.5 eV and 5.0 eV. The surface-related states are thus expected to be very sensitive to various surface phases.[26] In this perspective, we look at the 2.1-ML Sb covered (1×1) phase, Fig. 5(g), which shows a bulk-plasmon peak at the energy value of 16.7 eV and a 5*s* shallow core level at 6.3 eV.[27] In the temperature range from RT to 350° C as the Sb adatoms agglomerate on a stable Sb monolayer, where the (1×1) LEED sharpens, the EELS features show an enhancement of the surface plasmon while the peak at about 6.3 eV broadens. At higher temperatures when 0.85 ML of Sb results in a $d(2\times1)$ phase, Fig. 5(e), the EELS is essentially like that of the (1×1) phase. For lower coverage phases this 6.3-eV peak sharply decreases in relative intensity and shows two small peaks in this region for (5×5), $(\sqrt{3}\times\sqrt{3})$, and $(5\sqrt{3}\times5\sqrt{3})$ phases. Meanwhile the surface-plasmon peak at 11.0 eV begins to decrease again. For the 0.33-ML $(\sqrt{3}\times\sqrt{3})$ phase, Fig. 5(c), and the 0.2-ML $(5\sqrt{3}\times5\sqrt{3})$ phase, Fig. 5(b), all the peaks except the bulk plasmon at 17.3 eV shrink, indicating a large scattering in these $\sqrt{3}$ symmetry surface phases. Also, it is interesting to note that in these two phases the 14.5-eV and 8.0-eV peaks, which are related to the surface states of the (7×7) structure, are prominent here. However, on annealing to 880° C the clean Si(111) surface, Fig. 5(a), is recovered revealing the strong 17.5-eV and 11.0-eV bulk- and surface-plasmon peaks. The observation that the bulk EELS feature does not show any significant change during the thermal annealing while the surface-related features are sensitive suggests the influential role of the rearrangement of surface adatoms, as manifested in LEED. We can observe that the nonrotated integral reconstructions such as the (1×1), $d(2\times1)$, and (5×5), show strong surface-plasmon features, while the 30° rotated $\sqrt{3}$ symmetry phases, such as the $(\sqrt{3}\times\sqrt{3})$ at 0.33 ML and the $(5\sqrt{3}\times5\sqrt{3})$ at 0.2 ML, show attenuation of the surface-plasmon and related peaks. Probably the symmetric arrangement of Sb adatoms on the (1×1) Si substrate in the (1×1), $d(2\times1)$, and (5×5), phases appears to assist the formation of surface electron collective excitations. The 0.4-ML (5×5) and 0.2-ML $(5\sqrt{3}\times5\sqrt{3})$ phases are novel phases observed during this desorption study and their detailed structures are yet to be determined. Elswijk *et al.*[13] have seen only small domains of the $(\sqrt{3}\times\sqrt{3})$ phase at 0.33 ML coexisting with (7×7) and disordered (7×7) phases. By scanning-tunneling microscopy they determine a simple Sb-adatom-based structure where the Sb adatom saturates the three dangling bonds by occupying the T_4 sites. However, we report here a long-range $(\sqrt{3}\times\sqrt{3})$ LEED (coherence length >100 Å), where we see the disruption of surface-plasmon and related features even in this 0.33-ML phase and also a strong 14.5-eV peak related to the surface state of (7×7). Since the $(\sqrt{3}\times\sqrt{3})$ 0.33-ML phase appears between the 0.4 ML (5×5) and the 0.2-ML $(5\sqrt{3}\times5\sqrt{3})$ phases, showing features of the DAS structure and disrupted surface-plasmon peak, we suggest that the atomic arrangement in this phase obtained by the desorption route could be different from the previous model for the 0.33-ML $(\sqrt{3}\times\sqrt{3})$ phase. However, a more direct method of determining the atomic arrangement is essential to conclusively understand the reconstructions and their energetics.

IV. CONCLUSIONS

In summary we have studied the thermal stability of the Sb/Si(111) interface formed at RT which demonstrates the influence of growth kinetics on the geometric arrangement and consequently on the electronic properties. We observe that annealing the RT deposited (1×1) phase causes the Sb adatoms to agglomerate into large islands, with a small activation energy. Above 350° C, the islands desorb leaving a stable (1×1) Sb monolayer. At higher temperatures, the monolayer desorbs via several long-range symmetric phases as seen by LEED. The desorption route starting from the (1×1) 1.0-ML phase shows the formation of $d(2\times1)$, (5×5), $(\sqrt{3}\times\sqrt{3})$, and $(5\sqrt{3}\times5\sqrt{3})$ phases, while starting from a $(\sqrt{3}\times\sqrt{3})$ 1.0-ML phase it adopts a different route. The EELS studies of all these stable superstructures suggest the difference in electronic structure. The desorption sequence and similarity in EELS features in the 0.33-ML $(\sqrt{3}\times\sqrt{3})$ and the 0.2-ML $(5\sqrt{3}\times5\sqrt{3})$ phases suggest an energetically proximal arrangement for these phases. The fact that several phases, such as the 1.0-ML $(\sqrt{3}\times\sqrt{3})$ and 0.5–0.7-ML $(5\sqrt{3}\times5\sqrt{3})$, obtained by adsorption at respective temperatures are not traced in this desorption study sug-

gests several energy minimization pathways, depending on the kinetics of growth and the dynamics of desorption. This work is expected to stimulate further detailed local-order atomic arrangement studies and theoretical calculations to understand the actual relationship between the geometric and electronic structures, determined by the kinetics.

ACKNOWLEDGMENTS

The authors gratefully acknowledge the encouragement of the Director, National Physical Laboratory. One of the authors (S.M.S.) thanks the Department of Science & Technology, New Delhi, for financial support.

*Fax: +91-11-5726938. Email address: prasad@csnpl.ren.nic.in

[1] V. G. Lifshits, A. A. Saranin, and A. V. Zotov, *Surface Phases on Silicon* (Wiley, New York, 1994).
[2] S.M. Shivaprasad, T. Abukawa, H.W. Yeom, M. Nakamura, S. Suzuki, S. Sato, K. Sakamoto, T. Sakamoto, and S. Kono, Surf. Sci. **344**, L1245 (1995).
[3] S.M. Shivaprasad, C. Anandan, S.G. Azatyan, Y.L. Gavriljuk, and V.G. Lifshits, Surf. Sci. **382**, 258 (1997).
[4] S.M. Shivaprasad, Y. Aparna, and S. Singh, Solid State Commun. **107**, 257 (1998).
[5] S. Singh, S.M. Shivaprasad, and C. Anandan, Appl. Surf. Sci. **152**, 213 (1999).
[6] H.J. Gossmann and E.F. Schubert, Crit. Rev. Solid State Mater. Sci. **18**, 1 (1993), and references therein.
[7] H.P. Zeindl, T. Wegehaupt, I. Eisele, H. Oppolzer, H. Reisinger, G. Tempel, and F. Koch, Appl. Phys. Lett. **50**, 1164 (1987).
[8] A.V. Zotov, V.G. Lifshits, Z.Z. Ditina, and P.A. Kalinin, Surf. Sci. Lett. **273**, L453 (1992).
[9] M. Horn-von Hoegen, F.K. LeGoues, M. Copel, M.C. Reuter, and R.M. Tromp, Phys. Rev. Lett. **67**, 1130 (1991).
[10] M.I. Larsson, W.-X. Ni, K. Joelsson, and G.V. Hansson, Appl. Phys. Lett. **65**, 1409 (1994).
[11] Vinod Kumar Paliwal, A.G. Vedeshwar, and S.M. Shivaprasad, Surf. Sci. **513**, L397 (2002).
[12] C.-Y. Park, T. Abukawa, T. Kinoshita, Y. Enta, and S. Kono, Jpn. J. Appl. Phys., Part 1 **27**, 147 (1988).
[13] H.B. Elswijk, D. Dijkkamp, and E.J. Van Loenen, Phys. Rev. B **44**, 3802 (1991).
[14] S. Andrieu, J. Appl. Phys. **69**, 1366 (1991).
[15] K.H. Park, J.S. Ha, W.S. Yun, E.H. Lee, J.Y. Yi, and S.J. Park, J. Vac. Sci. Technol. A **15**, 1572 (1997).
[16] K.H. Park, J.S. Ha, W.S. Yun, and E.H. Lee, Phys. Rev. B **55**, 9267 (1997).
[17] Y.J. Ko, K.H. Park, J.S. Ha, and W.S. Yun, Phys. Rev. B **59**, 4588 (1999).
[18] A.A. Saranin, A.V. Zotov, V.G. Lifshits, O. Kubo, T. Harada, M. Katayama, and K. Oura, Surf. Sci. **447**, 15 (2000).
[19] S. Andrieu and F. Arnaud d'Avitaya, Surf. Sci. **219**, 277 (1989).
[20] Y. Enta, S. Suzuki, S. Kono, and T. Sakamoto, Phys. Rev. B **39**, 56 (1989).
[21] C. Argile and G.E. Rhead, Surf. Sci. Rep. **10**, 277 (1989).
[22] M. Stampanoni, A. Vaterlans, M. Aeschlimann, F. Meier, and D. Pescia, J. Appl. Phys. **64**, 5321 (1988).
[23] R.A. Metzger and F.G. Allen, Surf. Sci. **137**, 397 (1984).
[24] M.T. Cuberes, H. Ascolani, M. Moreno, and J.L. Sacedón, J. Vac. Sci. Technol. B **14**, 1655 (1996).
[25] J.E. Rowe and H. Ibach, Phys. Rev. Lett. **31**, 102 (1973).
[26] L. Pasquali, S. D'Addato, L. Tagliavini, A.M. Prandini, and S. Nannarone, Surf. Sci. **377-379**, 534 (1997).
[27] C.J. Powell, Proc. Phys. Soc. London **76**, 593 (1961).